MICROWAVE RESET–

A NEW METHOD FOR RESETTING A MULTIWELL JOSEPHSON PHASE QUBIT

by

Isaac Storch

A senior thesis submitted to the faculty of

University of California, Santa Barbara

in partial fulfillment of the requirements for the degree of

Bachelor of Science

Department of Physics

University of California, Santa Barbara

June 2009

UNIVERSITY OF CALIFORNIA, SANTA BARBARA

DEPARTMENT APPROVAL

of a senior thesis submitted by

Isaac Storch

This thesis has been reviewed by the research advisor and has been found to be satisfactory.

Date	John Martinis, Advisor

ABSTRACT

MICROWAVE RESET–

A NEW METHOD FOR RESETTING A MULTIWELL JOSEPHSON PHASE QUBIT

Isaac Storch

Department of Physics

Bachelor of Science

A new method for resetting a multiwell Josephson phase qubit using chirped microwaves is proposed and tested on a two well potential. It is postulated that the drive frequency should be a decreasing, linear function of time, based on simulations of a classical particle in a cubic potential well and qualitative observations of the "phase locking" phenomenon. An experiment is conducted to test the effect of a linear chirp on a qubit with the standard cubic potential. The chirp is generated using a Voltage Controlled Oscillator (VCO) and a Digital to Analog Converter (DAC). The output of the VCO can be measured by mixing it with a constant frequency signal and viewing the result on an oscilloscope.

The four parameters that characterize the linear chirp are the start frequency, end frequency, power, and duration. Data is presented showing the effect these parameters have on the probability that the particle will escape

from its initial well, and a calibration procedure is outlined. It is found that the end frequency does not affect escape probability as long as it is sufficiently low, and the start frequency serves as a switch that, when it is near the resonant frequency, causes the particle to escape. The power and duration are related by a phase locking threshold. Finally, the frequency selectivity of the chirp is found to be 100-500 MHz, and based on this information, we predict that we can reset a qubit with inductance as high as 5570 pH, corresponding to 11 wells.

ACKNOWLEDGMENTS

I would like to acknowledge the College of Creative Studies at UCSB for giving me a fantastic undergraduate education in physics and a fellowship for my first summer of research. I also acknowledge the Martinis Group, both current and former members, for their advice and support. And most importantly, I thank Professor John Martinis for providing me with such a challenging and interesting problem; I am extremely lucky to have been given a project like this as an undergraduate.

Contents

List of Figures

Chapter 1

Introduction

1.1 Background

Put simply, a quantum computer works by evolving an initial quantum state in time and then measuring the final state. Thus, no useful measurements can be made unless the quantum computer can be reliably reset into a known initial state; a requirement referred to as the second Divincenzo criterion. This paper explores a new reset method for a Josephson phase qubit with high inductance.

The Josephson phase qubit can be modeled by the circuit elements in Fig. 1.1. Physically, the Josephson junction (the 'X' symbol) consists of two superconducting wires separated by an insulator thin enough to allow electrons to tunnel across it. The voltage and current across the Josephson junction are given by

$$V_J = \phi_0 \dot{\delta} \qquad I_J = I_0 \sin \delta \tag{1.1}$$

where δ is the phase difference between the electron wavefunctions on either side of the thin insulator, I_0 is the critical current (current above which the junction starts behaving like a resistor), and $\phi_0 = \hbar/2e$ is a flux quantum. Using the junction rule

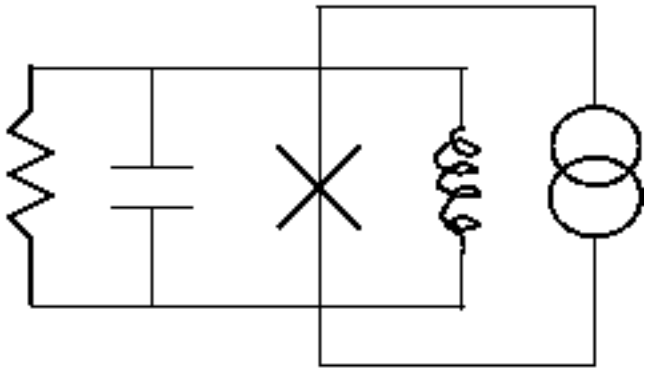

Figure 1.1 Josephson phase qubit circuit elements. The current source represents both the DC bias current and AC microwaves. The resistor is not part of the physical circuit; it is added to simulate energy decay

from basic circuit theory and setting the total current equal to an external drive gives

$$C\dot{V}_J + \frac{V_J}{R} + I_J + \int \frac{V_J}{L} dt = I_{drive} \tag{1.2}$$

Finally, substituting in the Josephson relations and multiplying (1.2) by ϕ_0 to get units of energy, one finds the classical Hamiltonian

$$C\phi_0^2\ddot{\delta} + \frac{1}{R}\phi_0^2\dot{\delta} + \frac{\partial}{\partial\delta}(-\phi_0 I_0 \cos\delta - \phi_0 I_{bias} + \frac{1}{2L}\phi_0^2\delta^2) = \phi_0 I_{drive} \tag{1.3}$$

The I_{bias} term, which came from an integration constant associated with the inductor element, can be thought of as a DC bias current. It is controlled by the magnetic flux from a coupled inductor and is thus proportional to the "flux bias", which is a term that will be used throughout the rest of this paper.

The expression in parenthesis is the potential energy of the system: a cosine plus a parabola. This potential provides a number of requirements for quantum computing, such as nonlinearity and a method for measurement. However, these details will not be discussed in this paper (see[1] for more information). Note that I_{bias} controls the location of the parabola's minimum and L is proportional to the "breadth" of the parabola. Thus, the higher the inductance, the more potential wells form (Fig. 1.2).

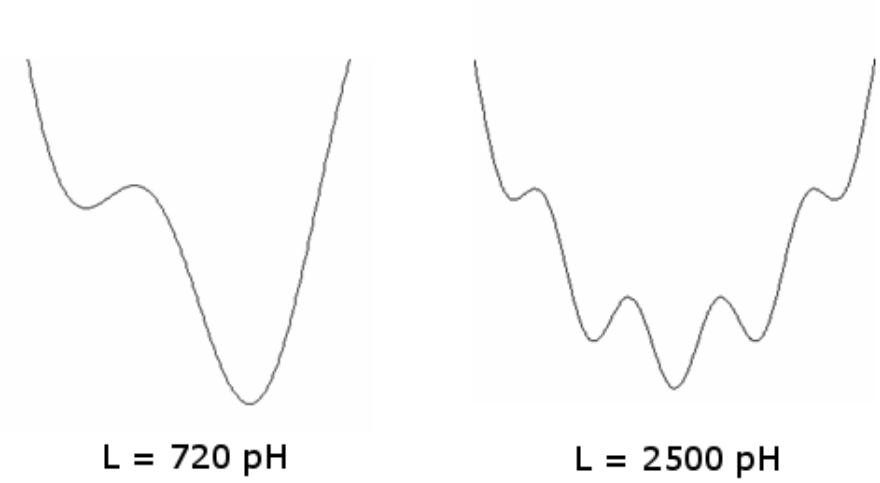

Figure 1.2 Potential for low and high inductance. The critical current is 2 μA. Note: the well height is not to scale between the two plots.

The reason we care about inductance in the first place is because it is directly related to flux noise. From electromagnetism

$$I_n = \Phi_n / L$$

where Φ_n is flux noise, and I_n is noise that appears in the I_{bias} term of the Hamiltonian given by (1.3). This type of noise vibrates the parabola, causing the $|0> \rightarrow |1>$ transition frequency to jitter, which makes the phase of the qubit state start to wander unpredictably. Again, details will not be given here, but the important thing to understand is that flux noise is related to the decoherence time T_2. Furthermore, flux noise is known to be independent of device parameters, such as inductance.[2] Thus, the higher the qubit inductance, the lower the effect that flux noise has on the qubit. However, increasing the inductance will make the qubit harder to reset.

Resetting a small L potential is fairly straightforward. One can usually find a flux bias value that will allow only one potential well. Shifting the flux bias to that value, allowing the qubit to decay to the bottom, and moving the flux bias back to

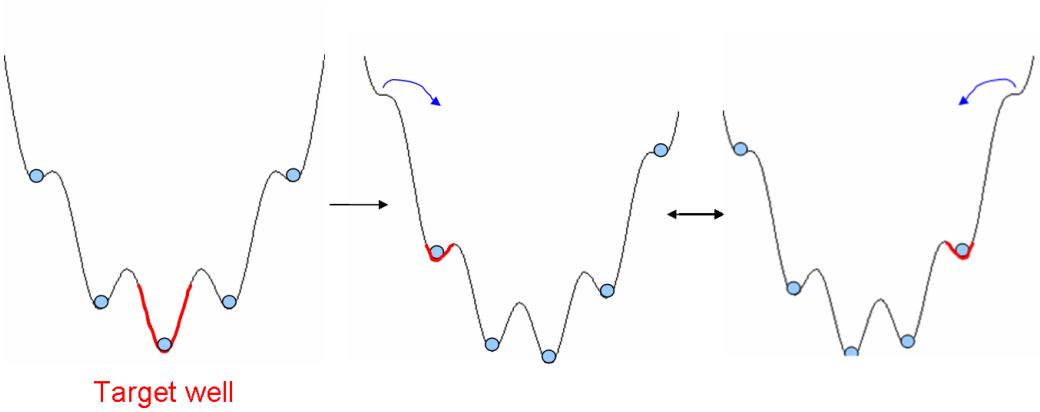

Figure 1.3 Illustration of tilting reset. The parabola is tilted left and right repeatedly, creating and emptying wells, but the target well is the only one that remains stable.

the operating point will provide 100% reset probability. However, a large L potential has many wells for all flux biases. Suppose we wanted to reset to the bottom well. We would first need to tilt the parabola far enough to the right to empty out all of the wells on the left, but then we would have created more wells on the right for the particle to be trapped in. The parabola would then need to be tilted all the way over to the left, and so forth. The target well is the only well that remains stable during this tilting procedure (Fig. 1.3), and with each tilt there is a relatively low probability the particle would get trapped in the target well, so it must be repeated. For a potential with 10 wells, 50 tilts would be required.[3]

At 10s of μs per tilt, the tilting method is not particularly efficient, but this paper explores a new method using microwaves that could make the reset for a multiwell potential significantly faster. Each well has its own resonant frequency, and a microwave signal could be used to drive all but the target well on resonance. Starting at the highest well, the particle could be driven out of each well in turn until finally relaxing into the bottom well. This method would be faster because no new wells are created, and each microwave signal would be about 10-300 ns in length. However,

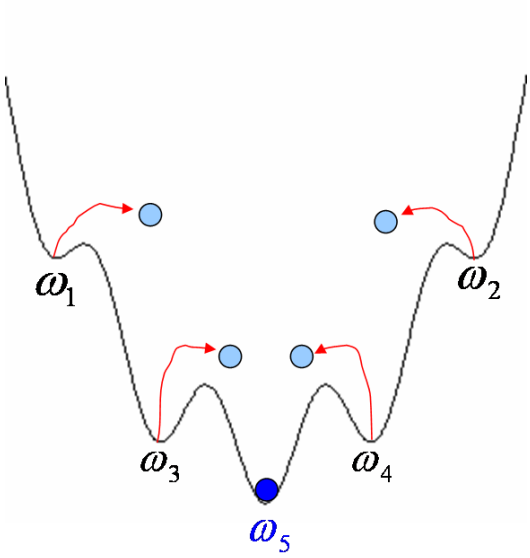

Figure 1.4 Illustration of microwave reset. The bottom well has a higher resonant frequency than all of the other wells, so the microwaves can be tuned to not excite the particle if it lies at the bottom.

the key to making this work is frequency selectivity. In general, deeper wells have higher resonant frequencies, and the bottom well is always the deepest. Therefore, the microwaves must be tuned to not excite frequencies above a certain value (Fig. 1.4).

1.2 Motivation for a Linear Chirp

A single well in Fig. 1.4 can be approximated by a cubic potential. For mathematical simplicity, we chose to simulate a potential of the form

$$U(\delta) = \delta^2/2 - \delta^3/3$$

which implies $\omega_p = 1$. The equation of motion was

$$\ddot{\delta} + \delta - \delta^2 = A \sin \phi(t)$$

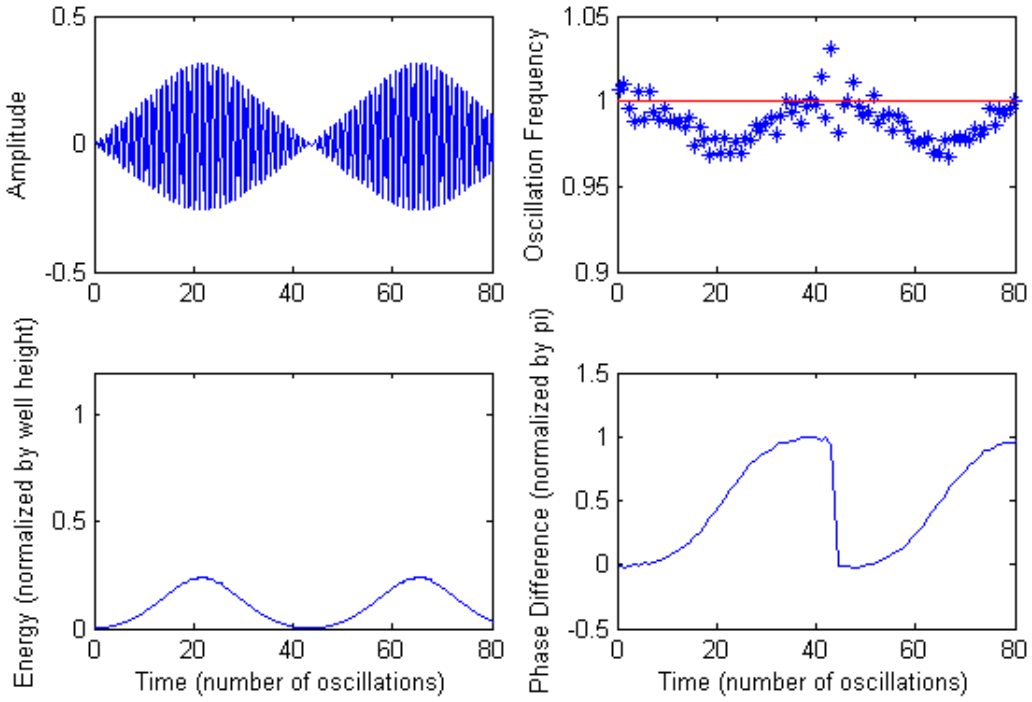

Figure 1.5 Simulated response to a constant frequency drive. Initially phase locked, but nonlinearity causes dephasing as the amplitude increases.

where the drive amplitude $A = 0.005$, which was chosen to be small compared to the barrier height $\Delta U = 1/6$ (experimentally we only care about the dynamics of low amplitude drives), and $\phi(t) = \int \omega(t)dt$ is the drive phase.

Figure 1.5 shows the response of the system to a constant drive frequency. The initial period where the phase difference is zero and the energy increases is known as "phase locking." Note that the initial increase in energy is quadratic in time, like that of the harmonic oscillator. However, as the particle's energy increases, the nonlinearity of the potential starts to take over and its oscillation frequency decreases, causing the drive to no longer be phase locked. Eventually, the drive is π out of phase and the particle is driven (harmonically) back to the bottom of the well, starting the process over again. If the drive frequency could match the particle's oscillation frequency for all time, the particle would eventually escape out of the well.

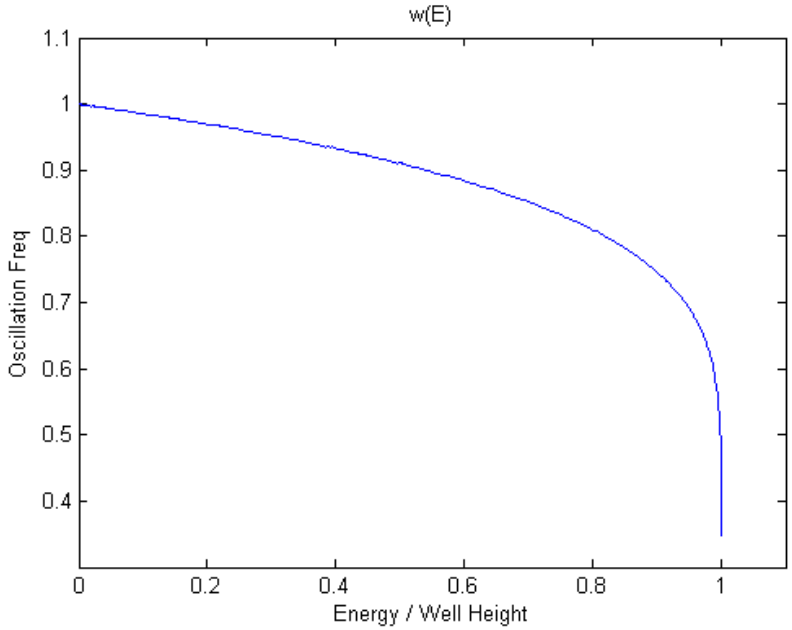

Figure 1.6 Nonlinear resonant frequency versus energy. Points on this curve are found by simulating the particle at some energy with no drive or decay, then finding the average frequency over several oscillations.

We can estimate what the frequency of the particle would be if it were driven on resonance for all time. By simulating the particle's oscillations at given energies with no drive and finding the average period, we can map out $\omega(E)$ (Fig. 1.6). Then, by assuming the energy increases quadratically with time, like that of the harmonic oscillator on resonance,

$$E = \frac{A^2 t^2}{8m}$$

we find $\omega(t)$ (Fig. 1.7). To take advantage of phase locking, we clearly want our drive frequency to decrease with time and in general follow some approximation of this curve. We refer to a drive frequency that changes with time as a "chirp".

Starting with the lowest order approximation, we simulated the system's response to a linear chirp (Fig. 1.8). Note that it succeeds in driving the particle out of the well where the constant drive frequency had failed. The chirp shown in Fig. 1.8 was optimized by MATLAB's fminsearch to drive the particle out of the well

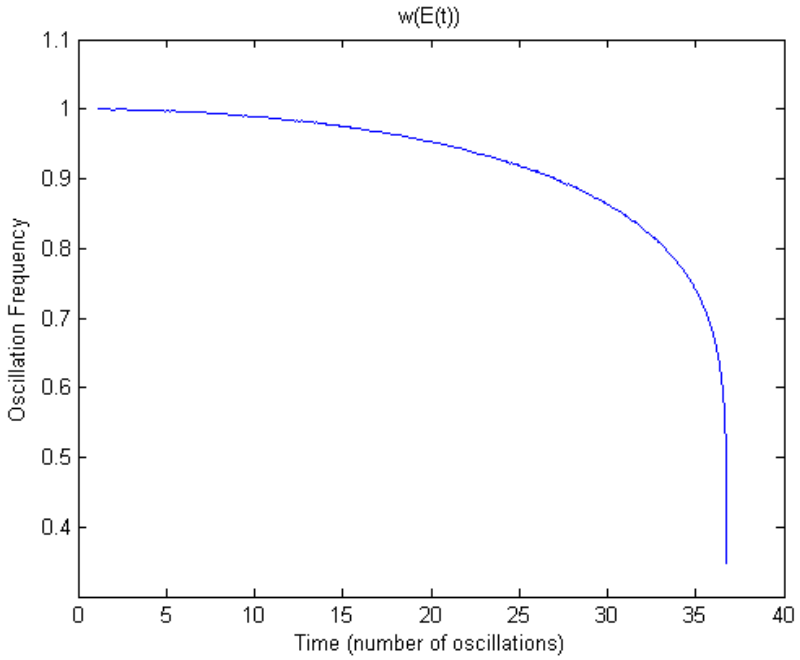

Figure 1.7 Ideal drive frequency function of time. If the drive frequency followed this $\omega(t)$, it would remain phase locked with the particle for all time and excite it resonantly.

in the shortest time. The particle remains phase locked longer than it does in Fig. 1.5 (a nonlinear phenomenon known as "autoresonance"), and even after losing phase locking, the energy oscillates and gradually increases until the particle escapes. These simulations motivate our experiment to see if linear chirps would be able to reset a Josephson phase qubit.

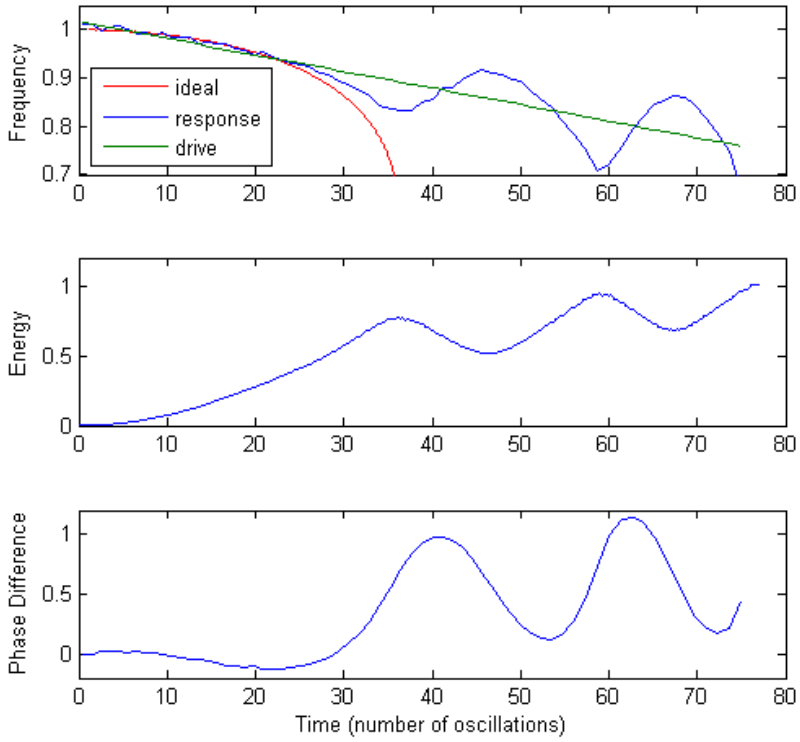

Figure 1.8 Simulated response to a linear chirp. Initially, $E \propto t^2$ like a harmonic oscillator, then it stops increasing because the drive loses phase locking. Note how the oscillation frequency follows the drive frequency even after losing phase locking, and the energy oscillates, but continues to increase.

Chapter 2

The Experiment

2.1 Setup

Consider the linear chirp in Fig. 1.8: it sweeps through 30% of its starting frequency in 80 oscillations. The duration of this chirp for a potential well with resonant frequency 8 GHz would be 10 ns. Thus, we needed to produce a microwave signal that sweeps through several GHz in 10 ns, which could not be done with any commercial generators we know of. The solution was to use a voltage controlled oscillator (VCO), which outputs a signal with a frequency proportional to an input voltage. The experimental setup is shown in Fig. 2.1.

We chose to use the Hittite HMC586LC4B VCO, which is specified for 4 - 8 GHz but was measured to have a range of 3.91 - 8.45 GHz. These frequencies correspond

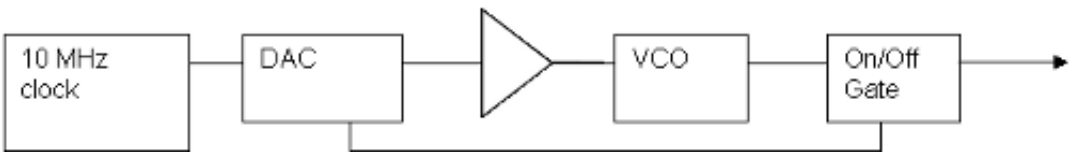

Figure 2.1 Experimental setup. Key components are a DAC board,[4] a custom amplifier, a custom VCO board, and an HP 11720A Pulse Modulator to gate the signal.

to a tuning voltage of 0 - 18 V, however, the digital to analog converter (DAC)[4] used to generate the voltage ramp can only output a voltage from 0 - 0.5 V. To get to the desired voltage range, an amplifier was designed using two high speed, high output voltage op-amps (Texus Instruments THS3001). The VCO itself came just as a chip, so a board was designed to house it, using proper microwave impedance matching techniques.

Using this setup, the deepest well that the particle could be successfully driven out of (80% probability) had a resonant frequency of 8.85 GHz. However, the resonant frequencies of the wells adjacent to the bottom well in a high inductance qubit can be as high as 12.5 GHz. Thus, an additional VCO with a range that extends to higher frequencies will most likely be needed in order for the microwave reset to work on a high inductance qubit.

2.2 Measuring the Output of the VCO

How to measure the rapidly changing output of a VCO is not immediately obvious, so we will outline the process here. We use a mixer to multiply the VCO output by a constant frequency sine wave from a signal generator and display the resulting signal on an oscilloscope (Figs. 2.2 and 2.3). The mixer output consists of the sum and difference of the two frequencies, and the oscilloscope filters out the sum component. Thus, the waveform will appear flat or slowly varying when the difference between the two frequencies is zero, oscillate faster when it is greater than zero, and finally get filtered out completely when it is much greater than zero. One can map out the frequency of the output versus time by manually incrementing the frequency of the signal generator and recording the time at which the two frequencies are equal. This was done for the data in Fig. 2.4, which shows the VCO's response to a step function.

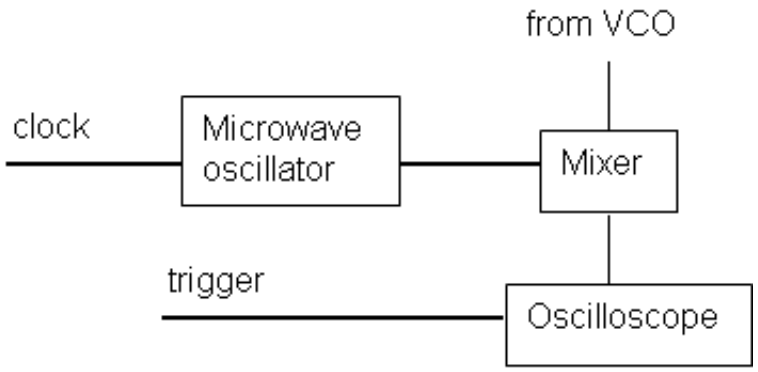

Figure 2.2 Setup to measure VCO.

We see about a 5 ns time constant for a changing output frequency, so the frequencies will follow our programmed values for the 10-300 ns chirps used in our experiment.

2.3 Procedure

The procedure for this experiment is fairly straightforward. We used a low inductance qubit with a two well potential and designated an initial well and a target well. The particle was then prepared in the initial well using the simple tilting reset described in §1.1, which has 100% probability of placing the particle in the desired well (again, only for sufficiently low inductance). Various linear chirps were applied, and the probability of the particle escaping from the initial well was measured.

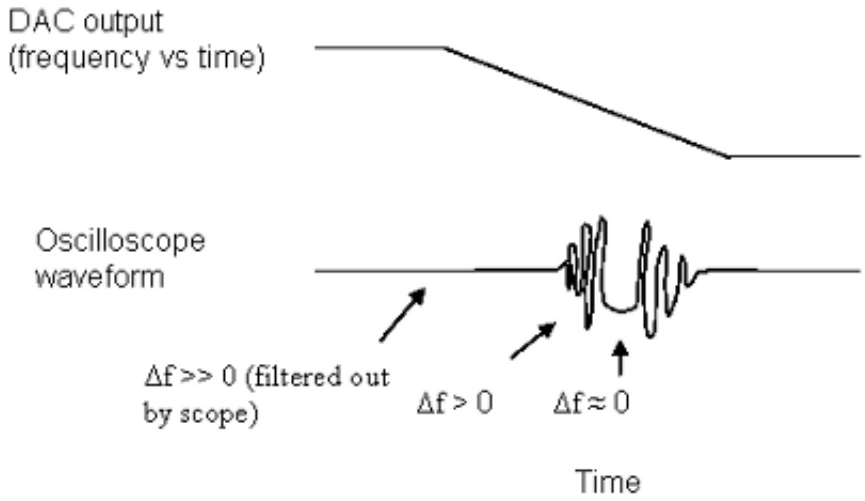

Figure 2.3 Oscilloscope waveform used to sample points for a frequency versus time plot of the VCO output.

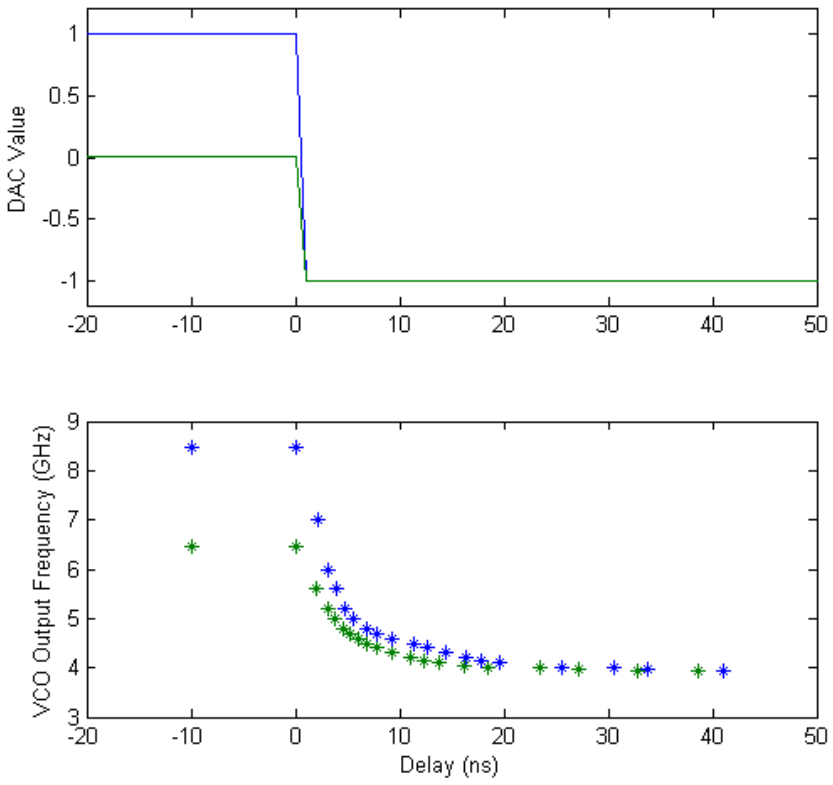

Figure 2.4 VCO step function response. Time constant is 5 to 10 ns.

Chapter 3

Data and Analysis

3.1 Chirp Parameters

The four parameters that characterize a linear chirp are start frequency, end frequency, power, and duration. The easiest way to understand how all of these influence the reset is to fix two of them and plot the other two as axes on a 2D color plot, where the escape probability is the color axis.

Figure 3.1 shows the data for fixing power and duration, while varying start frequency and end frequency. Several conclusions can be drawn from this plot. First, we succeeded at driving the particle out of the well using linear chirps, and second, downward chirps are more effective than upward chirps. The most effective chirps are those that start near the resonant frequency of the well, and also the end frequency has little effect so long as it is sufficiently low.

Now that we understand the start and end frequencies, we can fix them and vary the other two parameters. Figure 3.2 shows data for setting the start frequency near the resonant frequency and setting the end frequency low, while varying duration and power. Note that a threshold exists between parameter values that give high and low

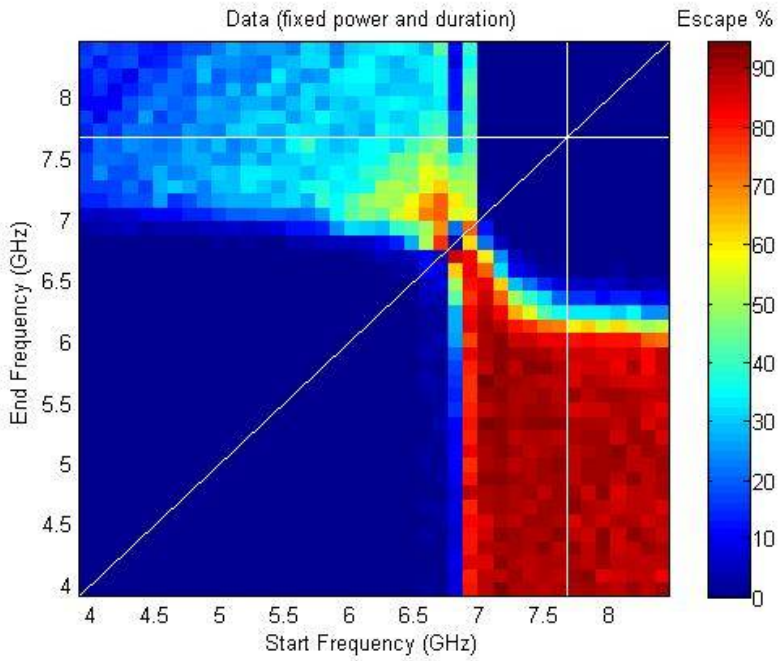

Figure 3.1 Escape probability versus start and end frequency. Attenuation = 7 dB, resonant frequency = 7.66 GHz, and duration = 100 ns. Lines mark the resonant frequency $\omega_p/2\pi$ of the cubic well.

escape probabilities. In other words, for a given duration, the chirp works at high power, but eventually stops working when the power is decreased below a certain level.

It is more enlightening to view these data on a log-log plot of drive amplitude versus chirp rate, with points marking 50% probability. Figure 3.3 shows the data plotted with simulations of the potential at different flux biases. The points tend to lie on straight lines, suggesting a power law. The positive slope makes sense intuitively: the higher the chirp rate, the more power is needed to cause autoresonance because the drive frequency is moving too quickly to "pick up" the particle. The form of this power law was found by Naaman et. al. to be $A_{threshold} \propto \alpha^{0.75}$ for a Josephson junction system,[5] where $\alpha = d\omega/dt$ is the chirp rate. However, a fit to the data in Fig. 3.3 suggests the scaling is $\alpha^{0.335}$, and our explanation for the discrepancy is that

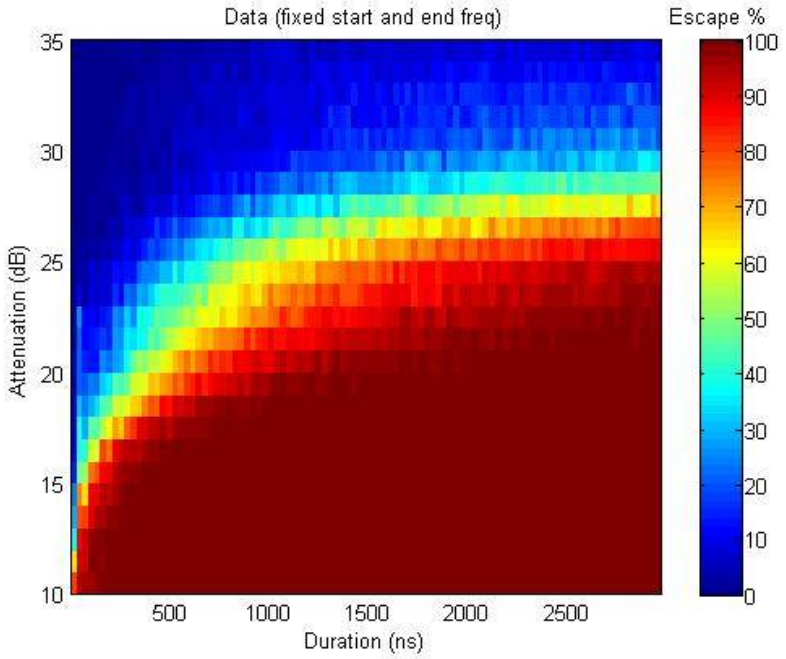

Figure 3.2 Escape probability versus power and duration. Start frequency = 6.86 GHz, resonant frequency = 6.34 GHz, and end frequency = 5.39 GHz. Note the phase locking threshold.

our potential is different and highly nonlinear. The simulations also show that this number changes with well depth, and can be tweaked enough to get 0.738. However, the most relevant information for this experiment is that a phase locking threshold exists and roughly follows a power law.

Based on this analysis, the procedure for tuning up a chirp would be something like the following. Set the end frequency as low as possible and guess where the start frequency should be, based on simulations; it should be low enough to not excite the bottom well, which has the highest resonant frequency. Choose the duration, keeping in mind that with everything else held constant, long chirps are more effective at exciting the particle than short chirps. Start at high power and see how well the reset works. If the reset probability is low, then tweak the start frequency up (in case it was not high enough to excite the wells near the bottom) and down (in case it was so

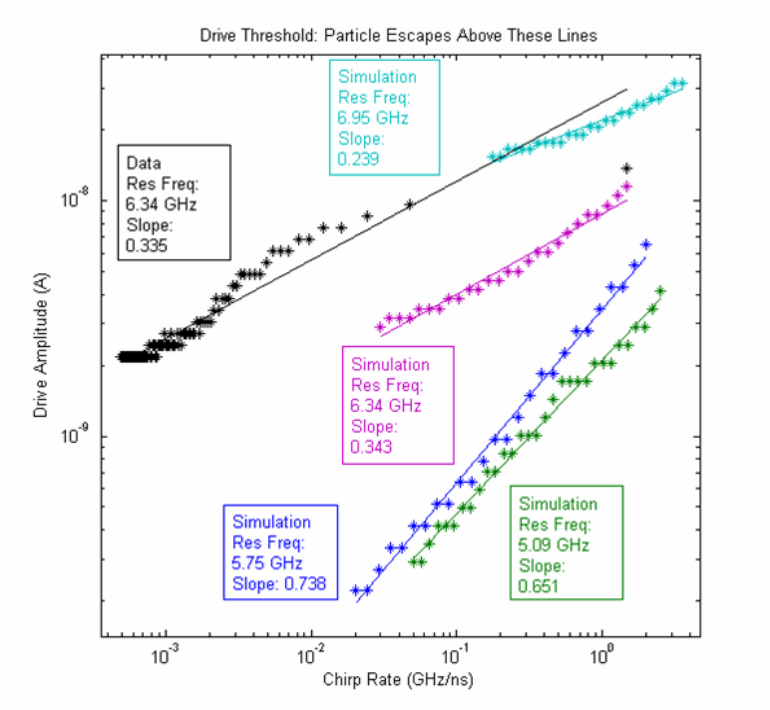

Figure 3.3 Drive amplitude versus chirp rate for data and simulations. The points mark the phase locking threshold, above which the particle escapes.

high that the bottom well was being excited), or choose a longer duration. If the reset probability is high, then decrease the power until it is just above the aforementioned amplitude-rate threshold.

The author feels that because a chirp calibrated to empty the deep wells should automatically empty the shallow wells, only one calibration is necessary. However, he suggests further investigation be done to see if a series of custom-tuned chirps for each well would be more effective than repeating the same chirp. Also, further research should be done to determine whether multiple short chirps are more effective than a single long chirp, and how the escape probability depends on the delay between chirps.

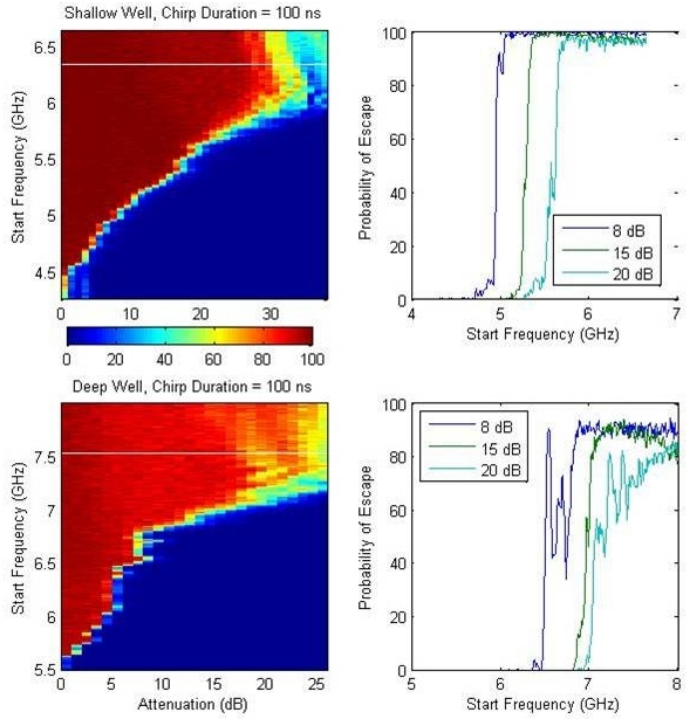

Figure 3.4 Escape probability versus start frequency and power. Resonant frequency for top plot = 6.33 GHz and resonant frequency for bottom plot = 7.52 GHz. Line cuts show frequency selectivity is 100-500 MHz.

3.2 Reset Efficacy

Of the four parameters discussed, the start frequency is most like the "switch" that determines whether the particle escapes from a particular well, based on how close it is to the resonant frequency. Consider Fig. 3.4, which shows how the escape probability varies with start frequency and power. Note that when the start frequency is too low, the escape probability is exactly 0% (not reset), and when the start frequency is close to the resonant frequency, it is greater than 90% (reset), but decreases with power. For the deeper well, "not reset" is still 0% and "reset" has lowered to about 80%. This implies that a deeper well is harder to reset, which makes sense.

A key issue to consider when projecting how this reset method will work on a multiwell potential is frequency selectivity; we need to know how far below the bottom

well's resonant frequency we can start the chirp and not excite the particle out of the bottom well. In other words, we must find the change in frequency from "reset" to "not reset". From the line plots in Fig. 3.4 we can see that the frequency selectivity is about 100 MHz, but can be as high as 500 MHz because of small peaks that form, which we do not understand. However, these peaks vanish at low power, so we can conclude that the frequency selectivity improves at low power.

In addition, Fig. 3.5 shows how the frequency selectivity changes with the resonant frequency of the well (i.e. well depth). There appears to be no correlation between the two; the frequency selectivity is still somewhere between 100 MHz and 500 MHz. However, note that the reset edge pulls in closer to the resonant frequency as the well gets deeper. Considering that the frequency of the bottom well is usually as high as 12-13 GHz, this implies that frequency selectivity alone determines how close we can set the start frequency to the resonant frequency of the bottom well without exciting it.

Now that we know the frequency selectivity, we can predict the highest inductance qubit that we can reset with this method. The standard two well potential has $L =$ 720 pH. A potential with $L = 2440$ pH has 5 wells and Δf, the difference between the frequencies of the two lowest wells, is 500 MHz; a potential with $L = 3910$ pH has 9 wells and $\Delta f = 200$ MHz, and a potential with $L = 5570$ pH has 11 wells and $\Delta f = 100$ MHz. Because the dephasing time T_2 scales as $\sqrt{L}$, being able to use the 11 well potential would increase T_2 by a factor of 2.78.

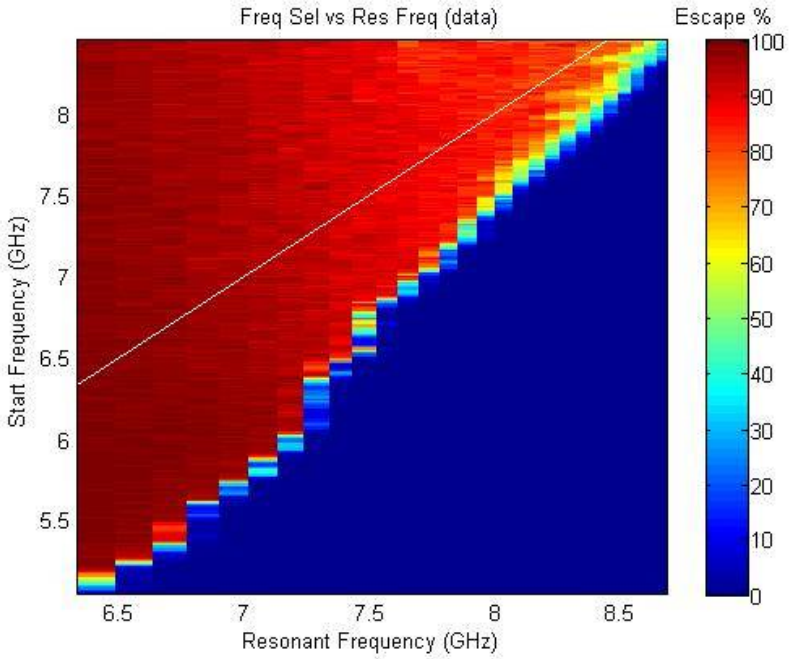

Figure 3.5 Escape probability versus start frequency and resonant frequency. Attenuation = 10 dB and duration = 100 ns.

Chapter 4

Conclusion

We have successfully demonstrated that linearly chirped microwaves can be used to reset a Josephson phase qubit. In addition, we understand how to optimize the chirp parameters to give a high escape probability with low power. This involves setting the start frequency near the resonant frequency, setting the end frequency as low as possible, and choosing power and duration near the phase locking threshold. We have determined the frequency selectivity of this method to be as low as 100 MHz, and predict that we can reset a qubit with $L = 5570$ pH. A qubit with this inductance would increase T_2 by a factor of 2.78.

Further research should be conducted in the following areas. Quadratic and parabolic chirps should be investigated because our simulations show that they might be more frequency selective than linear chirps (see Appendix B). A comparison should be made between using multiple short chirps and using one long chirp, and the dependence of the escape probability on the delay time between chirps should be analyzed. The phase locking threshold determined by the chirp's power and duration should be investigated more carefully, and a theory should be developed for the autoresonance of our specific system. Also, if a microwave reset is to work for a multiwell qubit, it

is likely that a VCO that reaches frequencies as high as 12.5 GHz will be needed. A method of stitching two chirps in different frequency ranges together might also need to be developed. Finally, the microwave reset must be applied to a multiwell qubit and compared with a tilting reset to see if it is indeed more efficient.

Bibliography

[1] John M. Martinis, "Superconducting Phase Qubits," Quantum Information Processing **8**, 81 (2009).

[2] Radoslaw C. Bialczak, R. McDermott, M. Ansmann, M. Hofheinz, N. Katz, Erik Lucero, Matthew Neeley, A.D. O'Connell, H. Wang, A. N. Cleland, and John M. Martinis, "1/f Flux Noise in Josephson Phase Qubits," Phys. Rev. Lett. **99**, 187006 (2007).

[3] T. A. Palomaki, S. K. Dutta, Hanhee Paik, H. Xu, J. Matthews, R. M. Lewis, R. C. Ramos, K. Mitra, Philip R. Johnson, Frederick W. Strauch, A. J. Dragt, C. J. Lobb, J. R. Anderson, and F. C. Wellstood, "Initializing the flux state of multiwell inductively isolated Josephson junction qubits," Phys. Rev. B **73**, 014520 (2006).

[4] John M. Martinis, "GHzDAC(FPGA) < Electronics < TWiki," https://commando.physics.ucsb.edu/tw/view/Electronics/GHzDAC(FPGA).

[5] O. Naaman, J. Aumentado, L. Friedland, J. S. Wurtele, and I. Siddiqi, "Phase-Locking Transition in a Chirped Superconducting Josephson Resonator," Phys. Rev. Lett. **101**, 117005 (2008).

Appendix A

Electronics

This appendix contains schematics and photos of the custom designed amplifier and VCO boards.

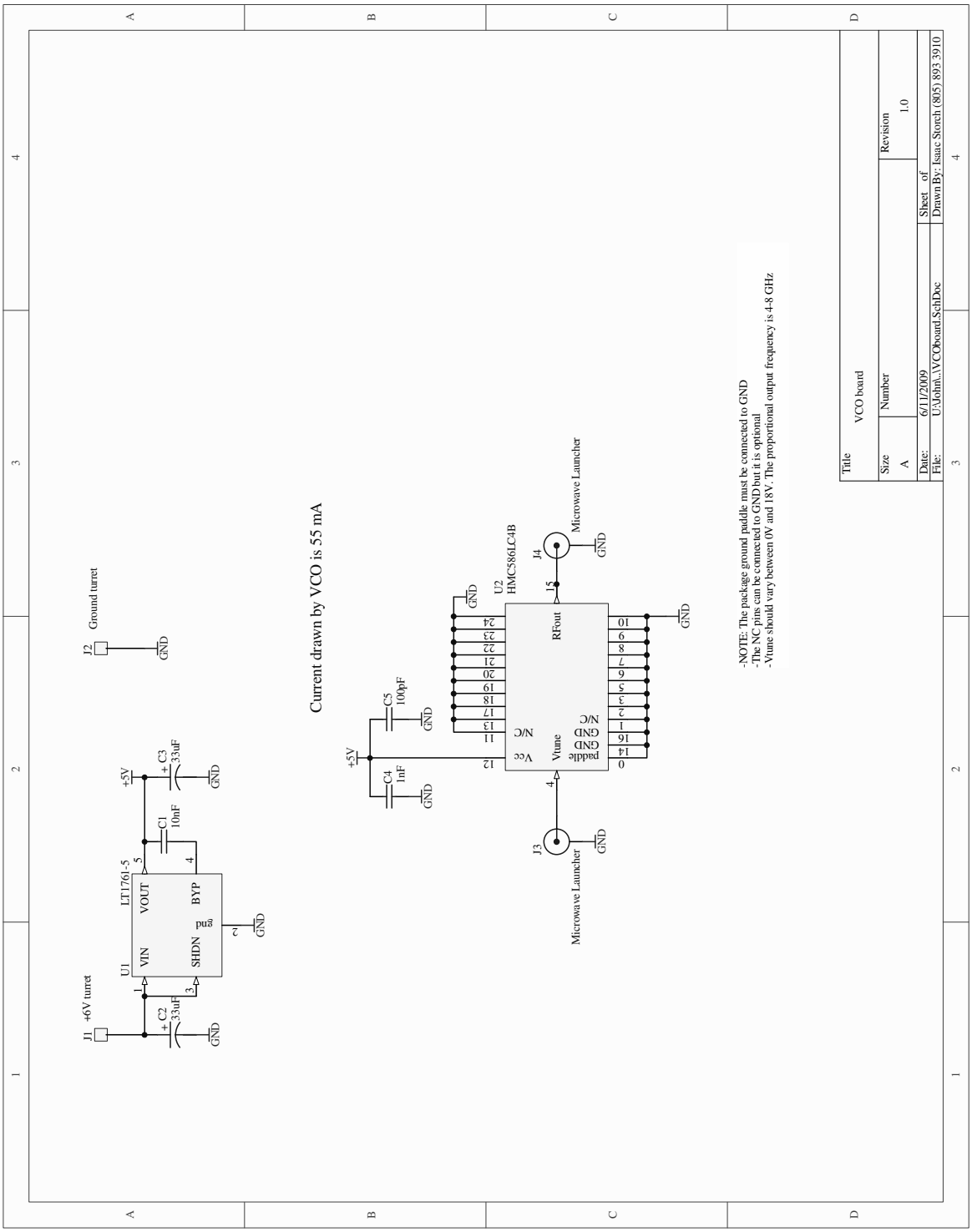

Figure A.1 VCO board schematic.

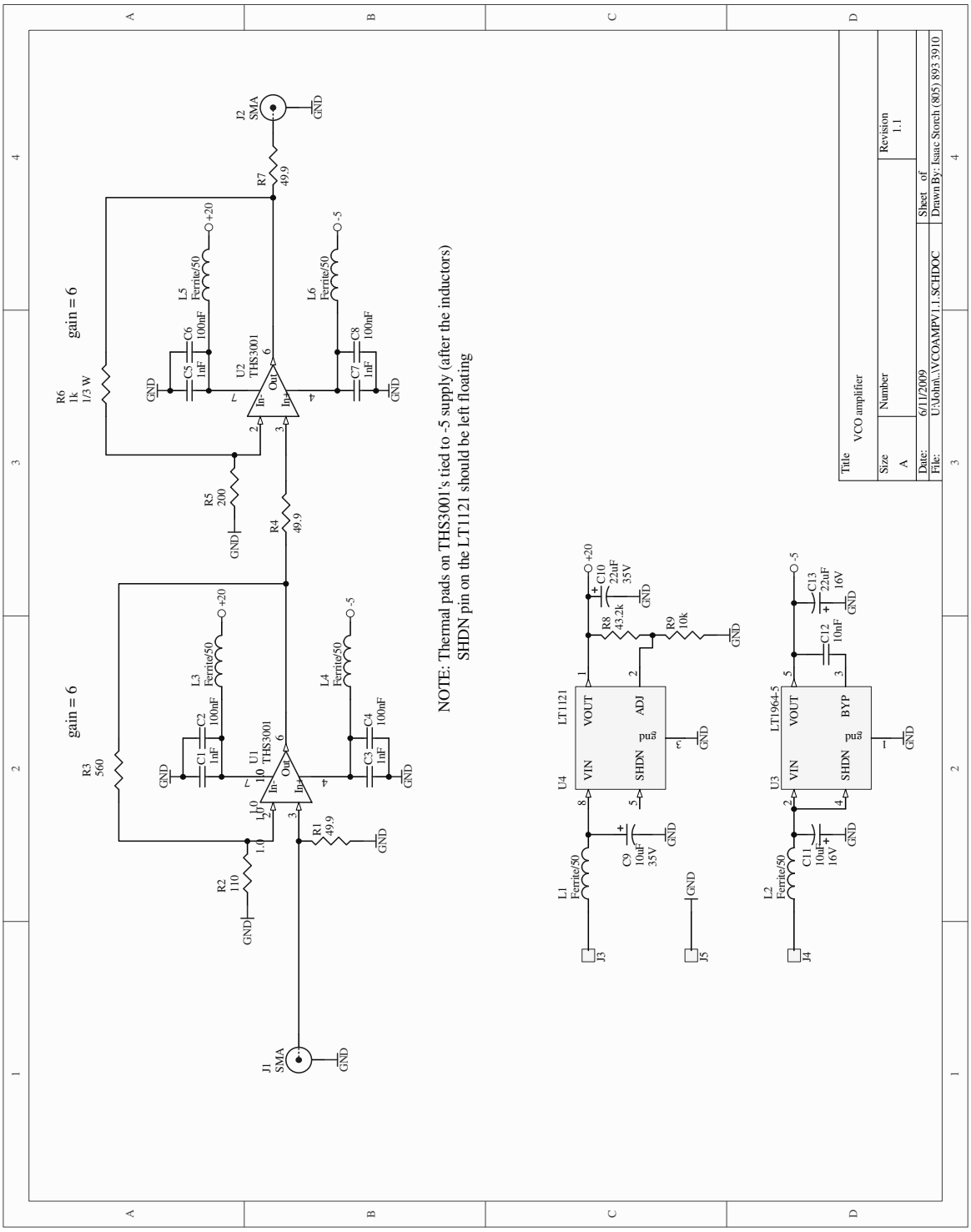

Figure A.2 VCO amplifier schematic.

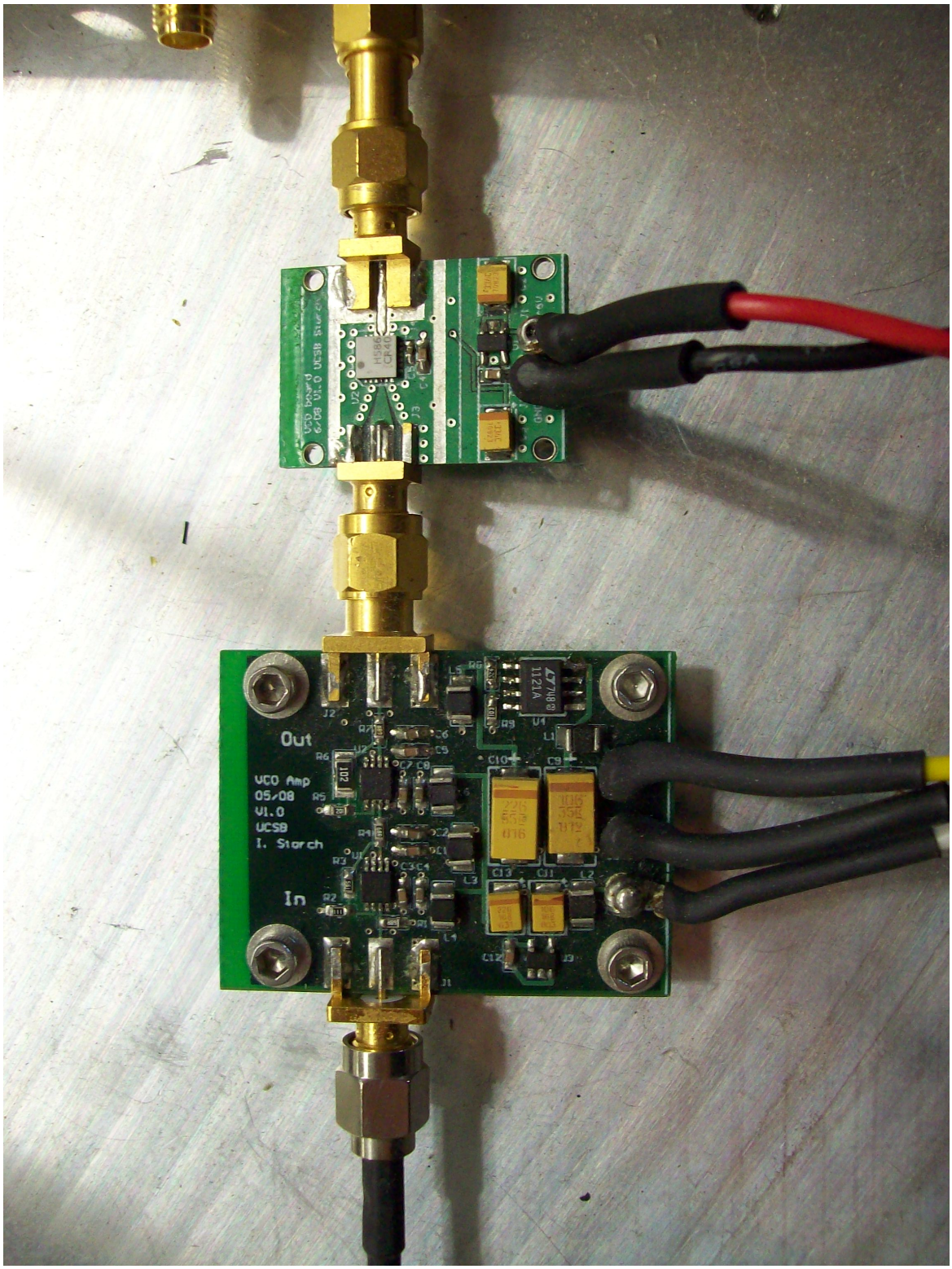

Figure A.3 Photo of the two custom boards.

Appendix B

Quadratic Chirp Simulations

This appendix contains a brief investigation into chirps other than linear functions of time. Figures B.1 and B.2 show the results of simulations on the cubic potential from §1.2 of a linear chirp, a quadratic chirp (defined by $\omega(t) = c_0 + c_1 t + c_2 t^2$), and a parabolic chirp (defined by $\omega(t) = c_0 + c_1 t^2$). Each of these chirps were optimized by fminsearch to make the particle escape in the shortest time: 77, 56, and 119 oscillations for the linear, quadratic, and parabolic chirps respectively (the ideal $\omega(t)$ given in Fig. 1.7 is 37 oscillations long). The change in frequency from $E = 0.1$ to $E = 1$ is 0.0208 for the linear chirp, 0.0328 for the quadratic chirp, and 0.0056 for the parabolic chirp. If the real potential well has a resonant frequency of 8 GHz, then this simulation implies that a linear chirp should have a frequency selectivity of 166 MHz. This is within the range found in §3.2, which suggests these simulations are reasonable.

Note that the quadratic chirp actually worsens frequency selectivity (increases Δf) by a factor of 1.58, while the parabolic chirp improves it (decreases Δf) by a factor of 3.71. This is surprising because the quadratic is a better approximation of the ideal $\omega(t)$ curve. Also note that the parabolic chirp takes the longest amount of

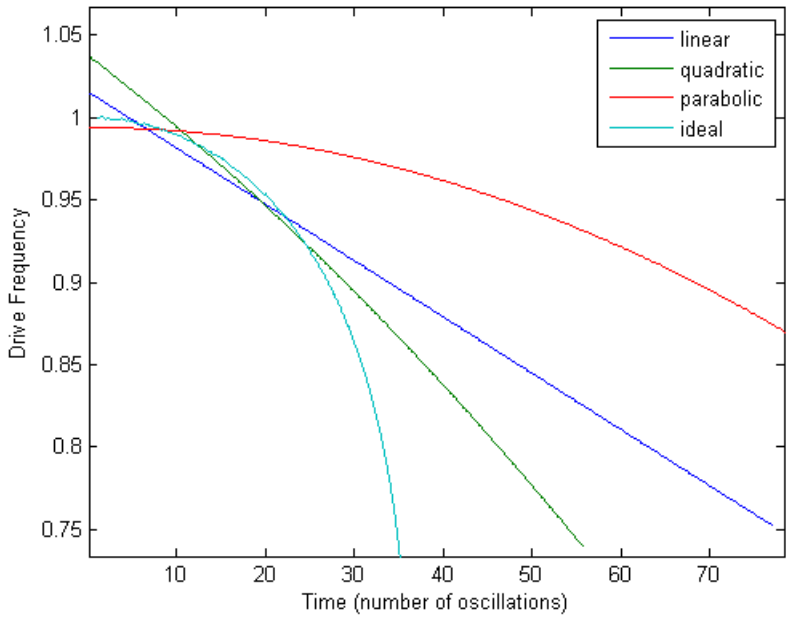

Figure B.1 Plot of various drive frequency functions. All drive frequency parameters were found with MATLAB's fminsearch.

time to cause the particle to escape. However, the frequency selectivity in Fig. B.2 is based on the maximum energy the particle obtains throughout the chirp, which may not directly correspond to the quantum mechanical probability of tunneling in the actual experiment. Also, fminsearch can only be used to find local minima, and it is quite possible that more optimal parameters for these chirps exist.

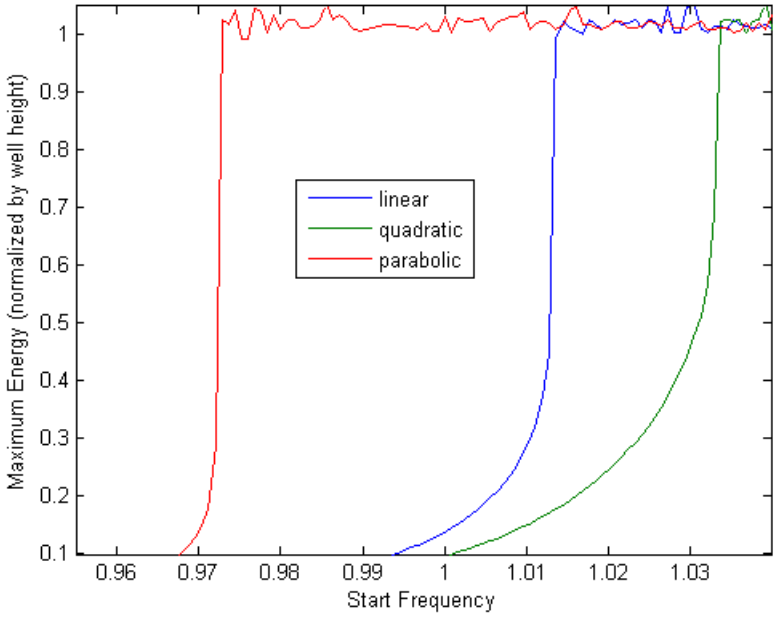

Figure B.2 Frequency selectivity of various types of chirps. The change in frequency from $E = 0.1$ to $E = 1$ is 0.0208 for the linear chirp, 0.0328 for the quadratic chirp, and 0.0056 for the parabolic chirp.